Geoscience Letters

RESEARCH LETTER

Open Access

Moho depth and tectonic implications of the western United States: insights from gravity data interpretation

Mohammad A. Shehata[1,2*] and Hideki Mizunaga[1]

Abstract

In this research, we figure out the lithospheric structures of the western U.S. and assess its tectonic implications with a high resolution using dense gravity data. Gravity data with high spatial resolution enables detailed mapping capabilities, overwhelming other geophysical data. To investigate the physical basis for support of topography in the western U.S., we employed the parker-Oldenburg algorithm to gravity to calculate the depth to Moho. The estimated depth to Moho shows an excellent spatial correlation with the physiographic provinces in the study area following an eastward thicking pattern. Moho of the stable craton reaches 50 km, whereas the western margin shows a shallow Moho of 20 km. Moreover, to assess the tectonic implication of Moho in the study area, we calculated the crustal compensation load to evaluate the isostatic state in the study area. The calculated compensation loads provide isostatic compensation for large-scale crustal structures, such as the broad, elevated Basin and Range Province. To assess the contribution of the crust and mantle to the topographic deformation in the study area, we calculated the crust topography and mantle topography. The Wyoming Craton and Great Plains have negative mantle topography values, contrasting with the relatively constant values in the southern Rockies, Colorado Plateau, and Basin and Range. Crustal topography reveals significant crustal support from the southern Rockies and the Wyoming craton. In addition, we estimated the lithospheric mantle thickness and the depth of the Lithosphere–Asthenosphere Boundary (LAB); the mantle thickness has values reaching 90 km at the stable eastern craton with LAB depth reaching 140 km. This research demonstrates the effect of the tectonic regime on the study area and the implications of this tectonic on the lithospheric structures with a high spatial resolution of a few hundred meters.

Keywords: Western Cordillera, Moho, Crustal Compensation Load, Residual Topography

Introduction

The development and evolution of the Earth's continental crust have far-reaching ramifications for tectonics, dynamics, and mass transport processes. Genuine concerns about the tectonic, melt, and volatile flux processes that build the crust continue to be one of the major research issues in the solid Earth sciences (DePaolo et al., 2008; Williams et al., 2010). Because of its greater buoyancy, the continental lithosphere is more resistant to subduction than the oceanic lithosphere. Because of its deformation resistance, the continental lithosphere has a longer and richer record of Earth's history than the seas. The North American Cordillera is the part of the American Cordillera that is situated in western North America. The Cordillera is a mountain range that extends parallel to the Americas' western coast. The North American Cordillera, also known as the Pacific Cordillera, encompasses much of western North America, including mountain ranges, intermontane basins, and plateaus (as well as much of the territory west of the Great Plains). The exact

*Correspondence: mohamed_shehata@sci.psu.edu.eg

[1] Department of Earth Resources Engineering, Faculty of Engineering, Kyushu University, Fukuoka 819-0395, Japan
Full list of author information is available at the end of the article

borders of the Cordillera depend on how each country defines it (Saager and Bianconi, 1971).

The western North America Cordilleran is an integral part of the Circum-Pacific orogenic belt, extending along a great circle path of about 25,000 km from the Antarctic Peninsula beyond Taiwan. The Cordilleran orogen's total length from the Gulf of Alaska to the mouth of the Gulf of California is about 5000 km, which is 20% of the orogenic belt. Subduction of oceanic lithosphere along the continental edges generated the geologic features of the Circum-Pacific orogenic belt. These spatially connected characteristics form an almost continuous chain along the Pacific coast (Fig. 1). The primary hallmarks of Circum-Pacific orogenesis in the geological record are the rock assemblages of subduction zones where oceanic plates are gradually devoured and the parallel magmatic arcs formed by linked igneous activity. The earliest rock assemblages show the Cordilleran continental margin. The boundary indicates the Cordilleran orogenic system's tectonic beginning in the mid-Early Triassic. Previous tectonic regimes of various features are recorded in older rock assemblages revealed within the mountain system. The Cordillera's tectonic evolution can be divided into seven stages: (1) formation of the continental margin in late Precambrian time and development of the Cordilleran passive margin, (2) brief orogenic events in the mid-to-late Paleozoic (Antler, Ancestral Rockies, and Sonoma orogenies), (3) the early Mesozoic "neutral" convergent margin (4) the beginning of the main Cordilleran orogeny in the Late Jurassic to Late Cretaceous, (5) the Laramide orogeny (Late Cretaceous to Eocene), (6) the mid-Cenozoic "ignimbrite flare-up," metamorphic core complexes, and (7) the Late Cenozoic Basin and Range rifting–San Andreas/Queen Charlotte transforms (Ostopowich, 2006). The core segment of the North American Cordillera, which encompasses the western half of the United States, is the subject of this study (Fig. 2).

Using densely recorded gravity data, we aim to determine the depth of the Moho interface in the research region. This estimate will result in a more detailed Moho map of the research region with significant lateral resolution. Furthermore, we assess the tectonic implications of Moho depth in the study area by calculating the crustal load and topographic origin in the study area.

Moho of the Western Cordillera

Several studies have looked at the Lithospheric structure of North America, focusing on the estimation of Moho depth. The researcher's activities generate a lot of attention in the western United States. These investigations mainly utilized data from the EarthScope national initiative, which produces enormous data for lithosphere research.

The NSF's EarthScope program uses hundreds of seismic, GPS, and other geophysical measurements to investigate the structure and development of the North American continent and the mechanisms that trigger earthquakes and volcanic eruptions. In 2003, work on this vital research center began. USArray is the keyEarthScope facility for Moho investigations, and it has generated hundreds of crustal thickness estimations using receiver function and tomographic analysis.

Various methodologies have investigated crustal structure in the western United States to find linkages between features and tectonic settings. These studies discovered specific tectonic provinces and terranes with significant

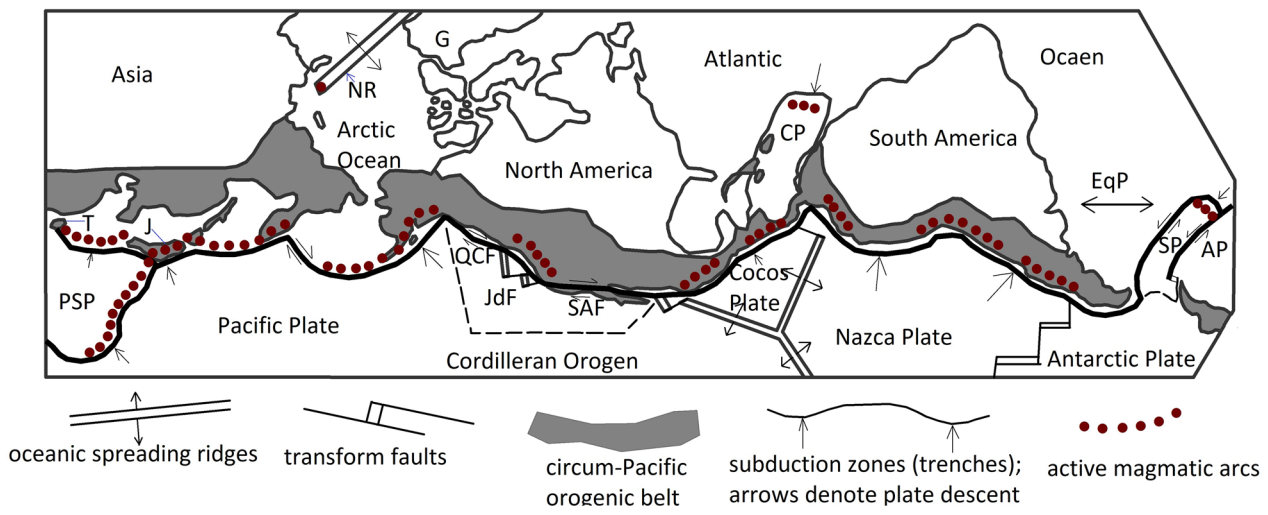

Fig. 1 Position of the Cordilleran orogen of western North America along the Circum-Pacific orogenic belt (Dickinson, 2004)

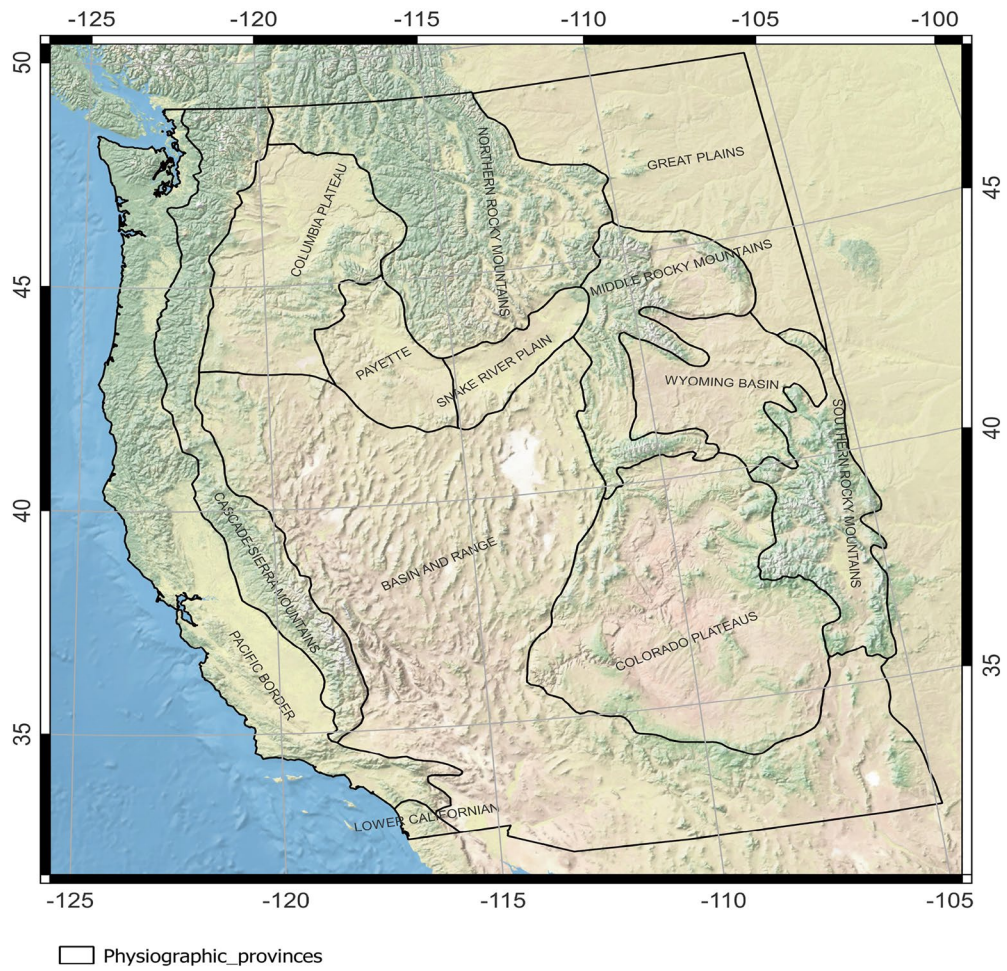

Fig. 2 Location map of the study area, western USA

variations in crustal thickness and changes in seismic velocities across the Moho in areas from the west coast of North America to the High Plains (Hansen, and Dueker, 2009; Buehler and Shearer, 2010; Eagar et al., 2011; Levander and Miller, 2012; Lin et al., 2014; Li et al., 2022).

Gilbert (2012) estimated the depth to Moho using the receiver function. He used a stacking method with bins whose radii were determined by the number of stations sampling a given region. This approach begins with a grid of uniformly spaced bins covering 2250 km in the north–south direction, 2100 km in the east–west direction, and a depth of 110 km, comparable to other standard conversion point stacking processes. Along the Colorado–Wyoming border, maximum thicknesses exceed 50 km. The southern Basin and Range in south Arizona contain a 30 km thick crust. The intensity of the colors corresponds to the receiver function's confidence in that location. The Moho depth is shown with full intensity in regions where it can be determined. Areas with more complicated receiver functions or lower amplitude signals that result in more uncertainty, on the other hand, are shown with less intense hues. The uncertainty scale ranges from full intensity plotting of locations where crustal thickness may be determined to within 1 km to faint hues plotting of places with 5 km or more uncertainties.

The depth of Moho in the western U.S. was measured by (Ma and Lowry, 2017) using the combined inversion of seismic receiver functions, gravity, and spatial statistics to determine the depth of Moho. Their findings revealed a regional crustal thickness of 38.9 km on average. Oceanic-derived accretionary terranes and excessively stretched lithosphere in rift zones are related to the thinnest crust in the west U.S. The Pacific coast, the southern Basin and Range province, the northernmost section of the northern Basin and Range, and the eastern and south margins of the Columbia Plateau all have thicknesses of less than 30 km. The crust under the Cascade

and Sierra–Nevada mountain ranges and the Snake River Plain is slightly thicker, ranging from 35 to 40 km thick. In the western United States, the Great Plains, middle and southern Rocky Mountains, Colorado Plateau, and Wyoming have the thickest crust (45–55 km).

Gravity data

The study area's gravity data came from the Bureau Gravimetrique International (BGI), founded in 1951 by the International Union of Geodesy and Geophysics (IUGG). The complete Bouguer gravity anomaly map (Fig. 3) was calculated as follows (g_{CBA}; Telford, 1990):

$$g_{CBA} = g_{obs} - g_t + (\Delta g_l + \Delta g_{FA} - \Delta g_B + \Delta g_T), \quad (1)$$

where g_{obs} is the station reading,Δg_{FA} is the free-air correction,Δg_l is the latitude correction, Δg_B is the Bouguer correction, Δg_T is the terrain correction and g_t is the theoretical sea-level gravity (also termed "normal gravity").

The usual representations of gravity data, such as maps and profiles, are dependent on the gravity adjustments employed. The phrase (gravity anomaly) is defined by subtracting the normal gravity value from all observed readings (Farag et al., 2022).

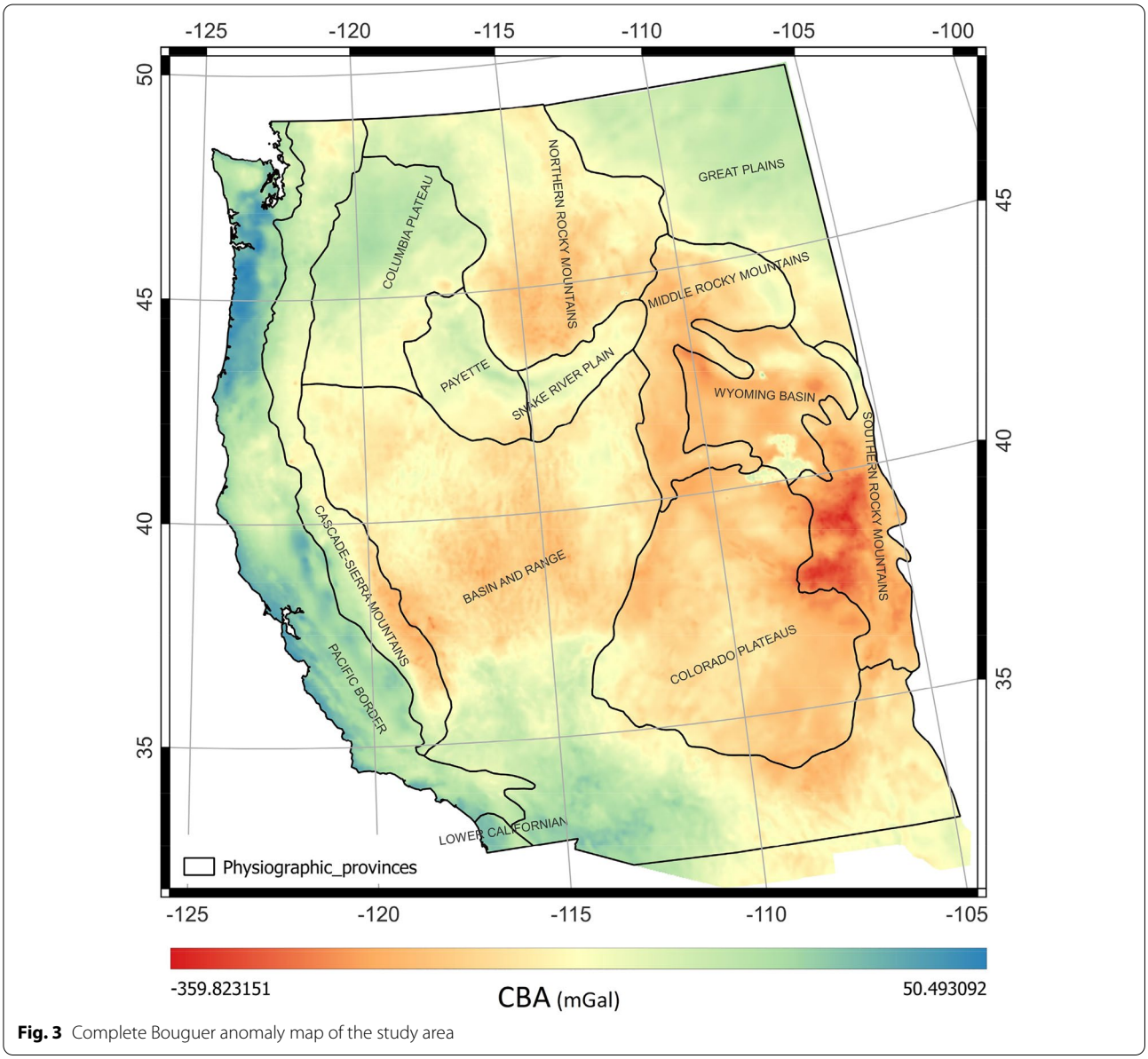

Fig. 3 Complete Bouguer anomaly map of the study area

Estimation of Moho depth

A typical difficulty of much geophysical research is mapping the three-dimensional density interface from the gravity anomaly. One such use is mapping crustal discontinuities from the gravity anomaly, such as the Mohorovicic discontinuity. The anomalies linked with these crustal discontinuities have been isolated using a variety of approaches (Chakraborty and Agarwal, 1992; Lefort and Agarwal, 2000). One of the critical goals in these instances is the inversion of the filtered gravity anomaly concerning the interface geometry.

Various approaches were presented to determine the geometry of a density interface connected to a known gravity anomaly (Rao and Babu, 1991). These methods use rectangular prisms with a constant density to approximate an undulating body. Each prism's gravity influence is computed, and the entire gravitational field is derived by summing the effects of all prisms. Tsuboi (1983) proposed a simple approach for computing the 3-D topography of a density interface based on a similar stratum methodology. Parker (1973) introduced Eq. (2) to estimate the gravity anomaly from an undulating interface by knowing the depth to the interface and the density difference across the interface. Parker's rearrangement of the forward algorithm was introduced by Oldenburg (1974). The Fourier transform of gravity anomaly, owing to the sum of the Fourier transforms of the powers of the bodies creating the anomaly, is the basis of Parker's procedure. Parker's expression might be adjusted to estimate the geometry of the density interface from the gravity anomaly, as Oldenburg (1974) proved.

Using a series of Fourier transformations, the inversion procedure calculates the gravity anomaly generated by an undulate, uniform layer of material using the equation presented by Parker (1973). This equation is defined as follows:

$$\mathrm{F}(\Delta \mathrm{g}) = 2\pi \mathrm{G}\Delta\rho e^{(-kz_0)} \sum_{n=1}^{\infty} \frac{K^{n-1}}{n!} F\left[h^n(x)\right], \quad (2)$$

where $\mathrm{F}(\Delta \mathrm{g})$ is the Fourier transform of the gravity anomaly, G is the universal gravitational constant, $\Delta\rho$ is the density contrast through the interface (Fig. 4a), K is the wavenumber, $h(x)$ is the depth to the density interface, and z_0 is the mean depth of the targeted interface.

Oldenburg (1974) rearranged Parker's equation to calculate the depth of the undulating interface using an iterative process as follows:

$$F[h(x)] = -\frac{F[\Delta g(x)]e^{(-kz_0)}}{2\pi G\Delta\rho} - \sum_{n=2}^{\infty} \frac{k^{n-1}}{n!} F\left[h^n(x)\right], \quad (3)$$

An iterative inversion procedure may be used to estimate the topography of the density interface using this formula.

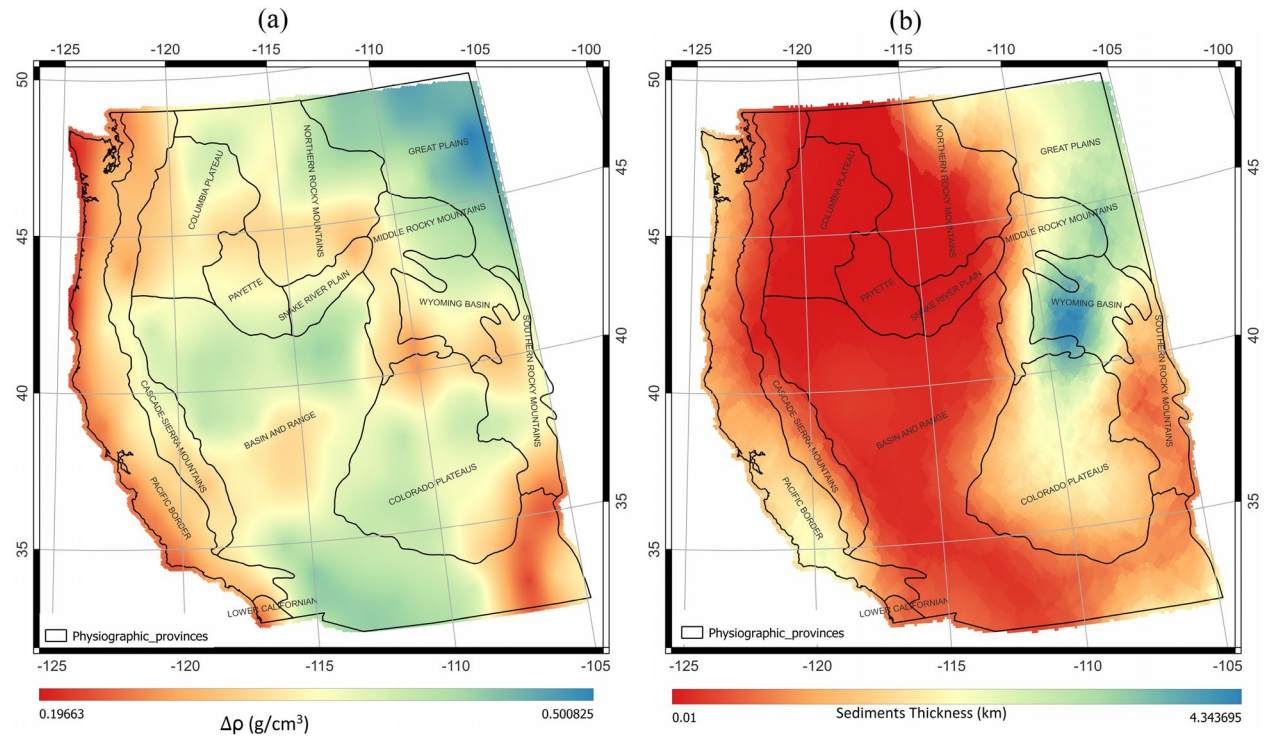

Fig. 4 **a** Density difference across the upper mantle and lower crust and **b** sediments thickness in the study area

Before computing the Fourier transform, the gravitational anomaly is first demeaned. The first term of Eq. (3) is then calculated by setting $h(x) = 0$. The initial estimate of the topographical interface is provided by Oldenburg (1974) and its inverse Fourier transform, h (x). This $h(x)$ value is then utilized in Eq. (3) to calculate a new estimate of $h(x)$. This procedure is repeated until a reasonable solution is found.

Because the depth to the interface is larger than zero and does not intercept the topography, Oldenburg (1974) deemed the process to be convergent. In addition, the amplitude of the interface relief should be less than the interface's mean depth. Because the inversion operation (Eq. 3) is unstable at high frequencies, the inversion process includes a High-Cut Filter, $HCF(k)$, to assure series convergence. The filter is described as follows:

$$\begin{aligned} &\text{for } WH < k < SH \\ &\rightarrow \quad HCF(k) = \frac{1}{2}\left[1 + \cos\left(\frac{k - 2\pi\, WH}{2(SH - WH}\right)\right], \\ &\text{for} \quad k > SH \quad \rightarrow \quad HCF(k) = 0, \\ &\text{for} \quad k < WH \quad \rightarrow \quad HCF(k) = 1, \end{aligned} \tag{4}$$

where WH and SH are predefined cutoff parameters.

This filter is used to restrict the high-frequency contents in the Fourier spectrum of the measured gravity anomaly. The frequency, k can be expressed as $1/\lambda$. λ is the wavelength in kilometers. The method iterates for a set number of iterations before stopping when the number of iterations is reached or when the difference between two subsequent topographical iterations is smaller than a pre-determined convergence threshold value. It is better to compute the gravity anomaly created by this computed tomography after the topographic relief has been estimated using the inversion approach. In general, this modeled anomaly should be identical to the input in the initial phase of the inversion process.

Isostatic equilibrium assessment

High-amplitude residual anomalies demonstrate that isostatic compensation for shallow density anomalies is not provided by variations in crustal thickness, as would be predicted by simple Airy or elastic plate models. To investigate this, we consider the crustal load, P, a quantity that characterizes the isostatic state of the lithosphere. It is equivalent to the sum of anomalous masses of the crustal column (Kaban and Mooney, 2001):

$$P = 2670t + (\rho_{sed} - 2700)s + \rho_{moho}(M_\circ - M), km.(kg/m^3) \tag{5}$$

where t is the topography (km), s is the thickness of the sedimentary basin (km) (Fig. 4b), ρ_{sed} is the average density of sediments (kg/m^3), M is the depth to Moho (km), $M_\circ = 25km$

All density values have units ($kg.m^{-3}$), and a value of 2670 $kg.m^{-3}$ is assigned for the onshore topography, 2700 $kg.m^{-3}$ for the standard upper crust, the density contrast across the Moho (ρ_{moho}) was estimated from the CRUST 1.0 model (Fig. 5a). P is equivalent to the thickness of a layer with a density of (±)1000 $kg.m^{-3}$ producing the same pressure as the lateral variations of the crustal model. Thus the residual topography, P, represents the mass that must be accounted for (added/subtracted) to the crust and upper mantle to provide isostatic equilibrium. Local features of P (for wavelengths < 100–150 km) are likely to be elastically supported by the lithosphere.

Residual topography

The orogen's elevation is frequently ascribed to a buoyant warm mantle. We investigated the origins of topographic relief in the western United States. The mean elevation (Fig. 5) of an isostatically balanced area may be thought of as a sum of contributions from the buoyancy of the crust H_c and the buoyancy of the mantle lithosphere H_m. We distinguished the contribution to topography ε from the crust H_c and that from the mantle H_m. Following (Lachenbruch and Morgan, 1990), we define the following:

$$\varepsilon = H_c + H_m - H_\circ \tag{6}$$

where the crustal and mantle contributions to buoyant height are

$$H_c = \frac{\rho_a - \rho_c}{\rho_a} L_c, \tag{7}$$

$$H_m = \frac{\rho_a - \rho_m}{\rho_a} L_m, \tag{8}$$

where ρ_c and L_c are the density and the thickness of the crust, respectively, and ρ_m and L_m are the density and thickness of the mantle–lithosphere, respectively. The crust and mantle densities were acquired from the CRUST 1.0 model. $H_\circ$ is a constant that allows the use of sea level as a reference datum. Lachenbruch and Morgan (1990) have further shown that a value $H_\circ = 2.4$ km makes Eq. 6 consistent with the density and elevations of mid-ocean ridges.

Because data constrain the thickness and density of the crust significantly more than the thickness and density of the mantle lithosphere, forecasting H_c is easier than estimating H_m in practice. Because the crust is lighter than the asthenosphere, H_c is always positive, but H_m is always negative, because the mantle lithosphere is heavier than the asthenosphere (same composition but cooler). If we believe

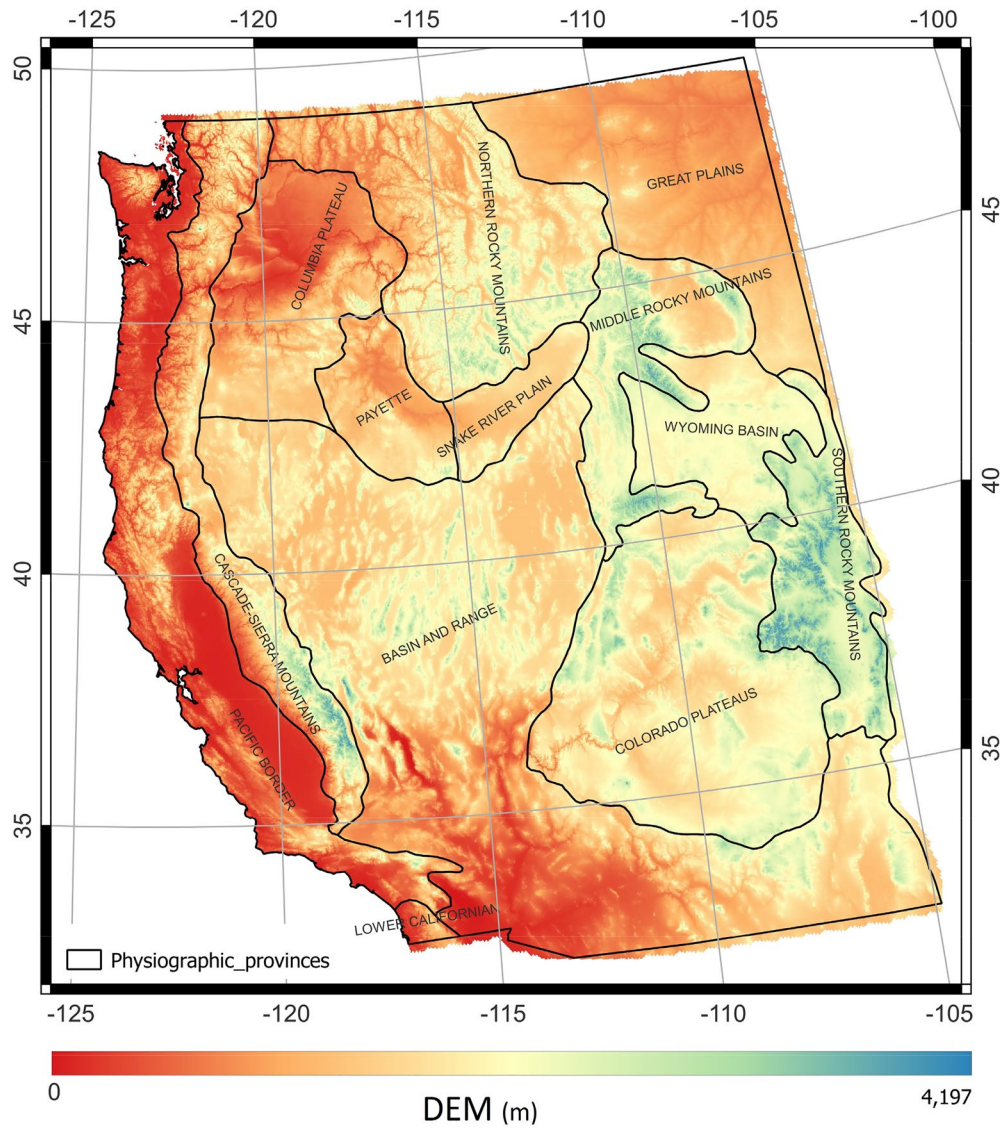

Fig. 5 Topography (m) in the study area

that residual changes in the Earth's topography that cannot be explained by variations in the crust's buoyancy are due to variations in the mantle's buoyancy, we may use Eq. 6 to compute H_m:

$$\mathrm{L}_m = \frac{\rho_a}{\rho_a - \rho_m}(\varepsilon + H_\circ - H_c) \tag{9}$$

where $\rho_a = 3200 kg.m^{-3}$ (Jones et al., 1992).

Results and discussion

Moho depth of the western USA

Moho depth map (Fig. 6) reveals depths ranging from 20 to 50 km. The Moho depth is characterized by an eastward thickening, with a thin crust on the western boundary. The Moho depth shows an excellent spatial correlation with the physiographic provinces in the study area. Deep Moho characterizes the study area at the east, whereas the eastern margin has a shallow Moho. The transition zone, Basin and Range, has a Moho depth of 30 km. The following sections provide a full explanation of Moho's depth in the study area. The Moho depth frequency (Fig. 7) illustrates that deep Moho is dominant in the area.

Western margin

Along the plate's western edge, in North America, there is a notable rise in crustal thickness between the coast and the arc. A shallow Moho may be seen on the western

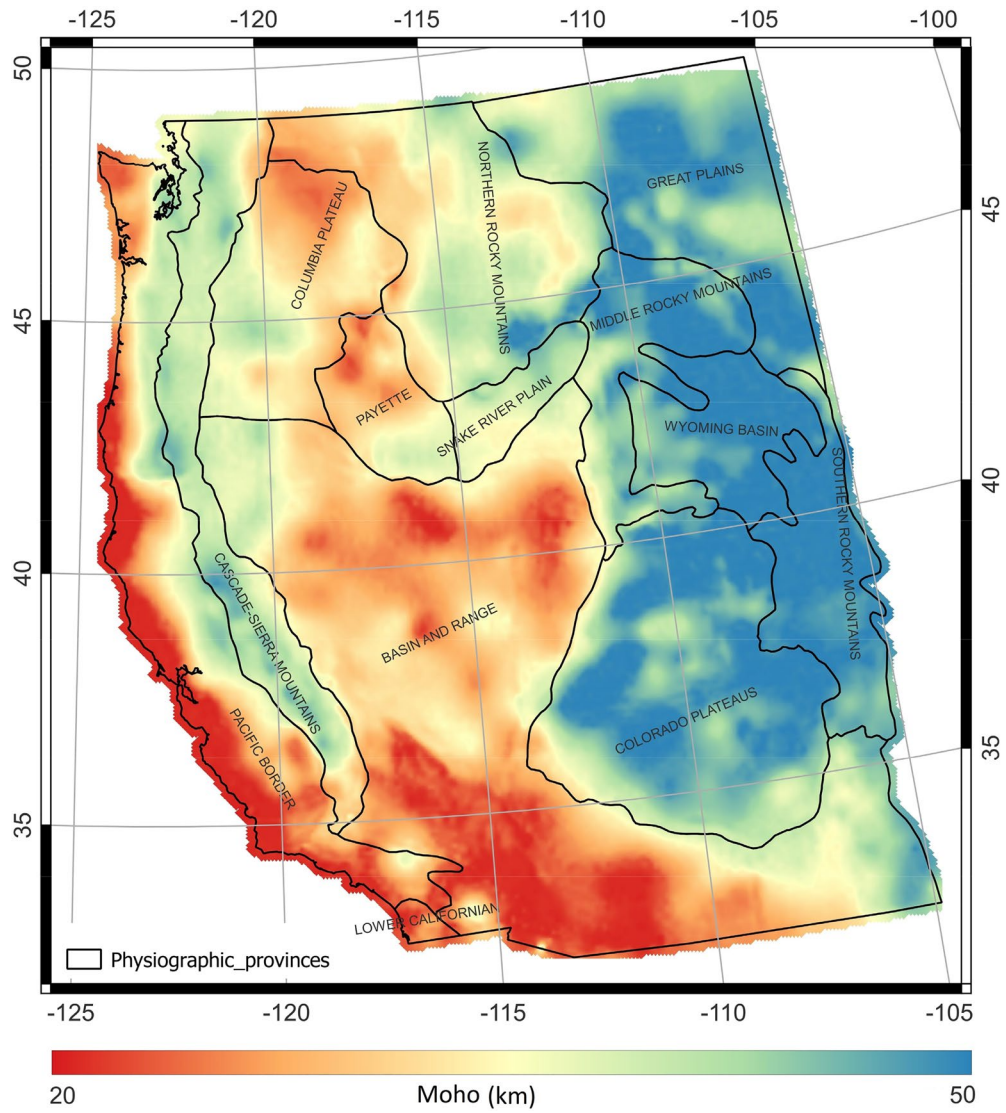

Fig. 6 Depth to the Moho interface map (km) in the study area

edge, with depths of 20 km. This shallow Moho shows the subduction zone of the Oceanic lithosphere beneath the continental crust.

Basin and range

Prior crustal thickness studies indicated the Basin and Range crust to be thinner than other sections of the western United States, confirming our findings. Normal faulting generated the usual regularly spaced mountain blocks separated by basins of the northern segment of the Basin and Range throughout much of Nevada during North America's western expansion (Zoback et al., 1981). The Basin and Range's northwestern part, which stretches from southern Oregon to northern Nevada, has crustal thicknesses of around 35 km. The crust thins to 30 km to the south of the northern limit of the Basin and Range in an east–west swath that runs through the northern part of Nevada eastward toward Salt Lake. At the eastern end of the Basin and Range and the Rocky Mountains in the north of Utah, the crust thickens substantially. The 30-km-thick crust in the northeastern Basin and Range Rocky Mountains changes to roughly 45 km towards the Uinta Mountains in the north region of the Wasatch Front.

Colorado plateau

The Colorado Plateau has a complex crustal structure that is restricted to the northwest and southeast by the thinning St. George and Jemez lineaments. The Colorado Plateau's crust is 50 km thick in the Rocky Mountains on

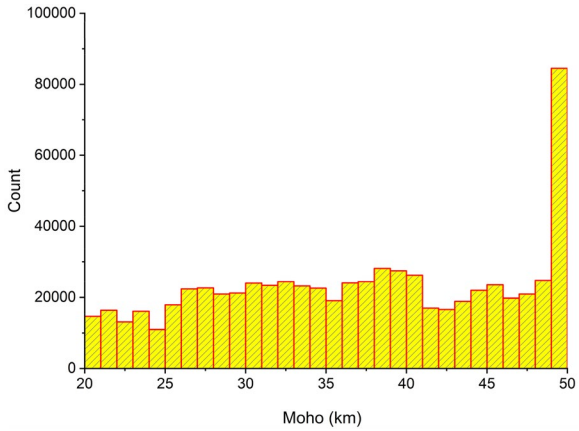

Fig. 7 Frequency distribution of Moho depth values in the study area

the east and 40 km thick near the Basin and Range on the west. Due to this gradient, it seems to represent a transitional zone between the heavier Rockies crust to the east and the thinner Basin and Range crust to the west. In the plateau's eastern and southern reaches, thicker crust zones depart from the main trend.

Snake River Plain

The Snake River Plain refers to a region 40 km southwest of Yellowstone's caldera where the crust hardens to a depth of 35 km. The Snake River Plain is made up of a sequence of caldera fields that started 16 million years ago in southwestern Idaho and northern Nevada at McDermitt caldera and extended eastward to Yellowstone caldera's most recent activity (Smith and Braile, 1994). The extensive volcanism in the Snake River Plain is produced by the entry of massive volumes of basaltic magma into the crust. As a result, crustal material melted, resulting in rhyolite lavas and ignimbrites erupting early. The crustal thicknesses of the Snake River Plain demonstrate a continuous zone of thickened crust, indicating that basaltic material thickened the crust over its whole length. The Bouguer gravity anomaly becomes less negative within the Snake River Plain, indicating less low-density crustal material and supporting the underplating of high-density material into the crust. This pattern differs from the High Lava Plains structure, owing to the patterns exposed by the focused deployment of the High Lava Plains (Eagar et al., 2011).

Rocky mountain and high plains

The Rocky Mountains are characterized by shortening-induced higher basement rocks, which show the extent of Laramide deformation eastward (Dickinson and Snyder, 1978). The structure of the Rocky Mountains crust alters as the range stretches north–south from Montana to northern New Mexico, as seen in the diagram above. In the Rockies near the Colorado–Wyoming border, the crust thickens to more than 50 km, making it some of the thickest crust in North America. To the north and south of this region, the Rockies' crust thins out, reaching barely 40 km in Wyoming, Montana, and New Mexico. According to previous research, the crust beneath the Rockies in northern Colorado is 50 km thick or more, and it is thinner to the north and south (Dueker and Sheehan, 1997; Gorman et al., 2002). Sharp elevations in crustal thicknesses have been seen along the western margin of the Colorado–Wyoming boundary, similar to the trend documented here.

We extracted three profiles trending east–west (Fig. 8) to reveal the variation in Moho depth across the transition zone. Profile (1) demonstrates the eastward thickening of the Earth's crust. The western margin shows a shallow Moho; east to the pacific border is the deep subduction trench adjacent to the shallow Columbia Plateau and Northern Rocky Mountain. Far east, the Great Plains has the deepest Moho. Profile (2) shows the same trend as profile (1), where the Basin and Range show a Moho depth that resembles the Columbia Plateau and Northern Rocky Mountains. Again, the far east shows the Moho depth of Wyoming Basin and Southern Rocky Mountain that correlate to the Great Plains. Profile (3) shows the varying Moho depth from shallow pacific border to deeper Basin and Range.

Isostatic State and Topography Origin

Additional compensatory loads occur throughout the crust and topmost mantle (Fig. 9). Large-scale crustal features, such as the vast, high Basin and Range Province, get isostatic compensation from these stresses. The shown values (m.kg/m^3) correspond to the thickness (in kilometers) of a layer having a density of 1000 kg/m^3.

In contrast to the largely constant values in the southern Rockies, Colorado Plateau, and Basin and Range, mantle topography estimations (Fig. 10a) suggest negative values in the Wyoming Craton and Great Plains. The crustal topography (Fig. 10b) shows that the southern Rockies and Wyoming craton provide major support.

Furthermore, our estimates of mantle–lithosphere thickness (Fig. 11a) revealed a variable mantle thickness reaching 65 km in the stable craton to the east of the study area. The mantle thickness correlates with the physiographic provinces in the study area where the Great Plains and the Wyoming craton have a thick mantle. In contrast, the Basin and Range have a thin mantle. The effect of mantle thickness on the Lithosphere–Asthenosphere Boundary (LAB) is shown in Fig. 11b, which is the combination of crust thickness

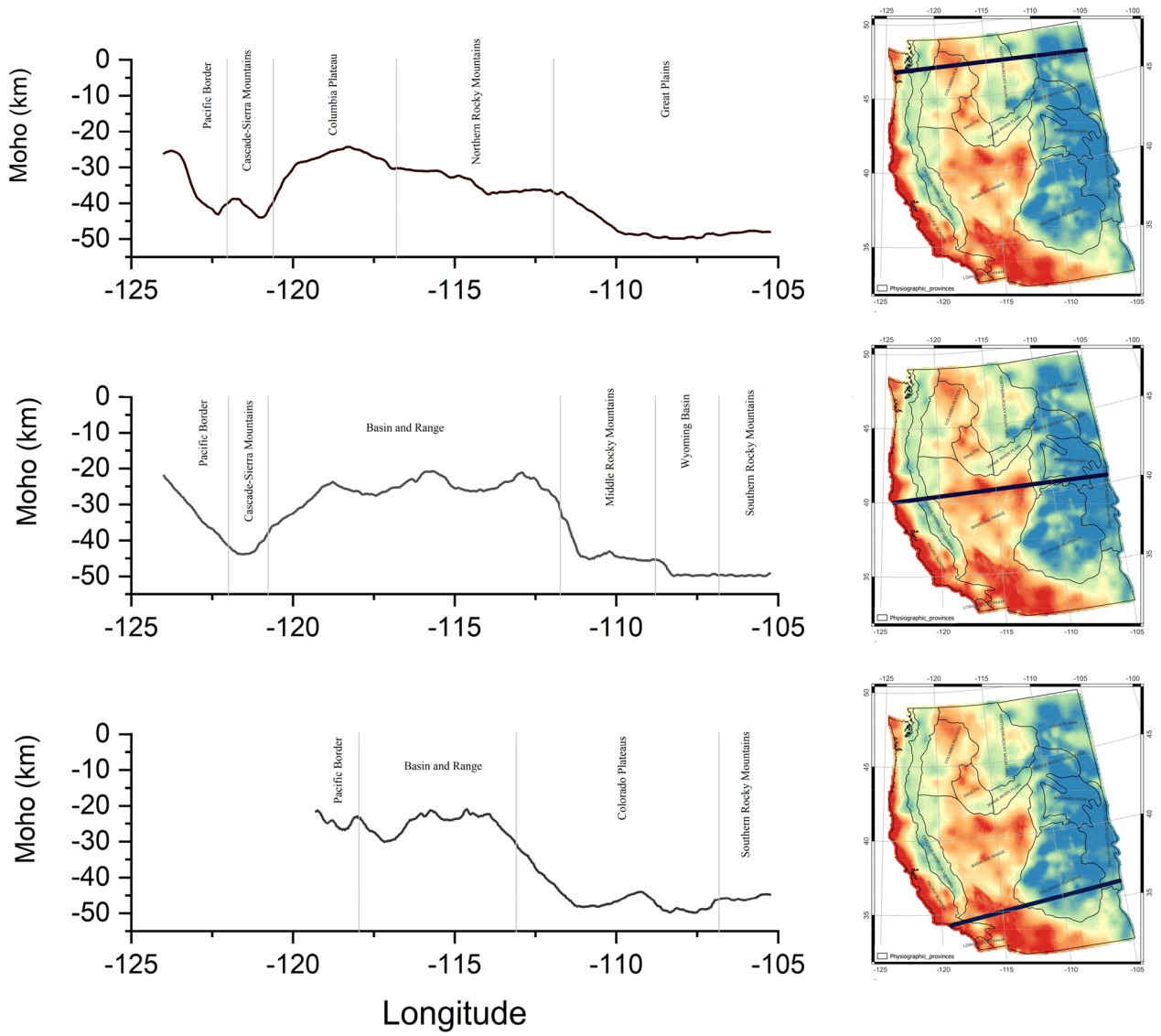

Fig. 8 Extracted east–west profiles in the study area

along with the lithospheric mantle thickness (Fig. 11a). LAB of the study area shows an excellent spatial correlation with the physiographic provinces and crustal thicknesses (Fig. 6).

Uncertainties and misfitting

To assess the accuracy of our calculations, we compared our estimates with the Moho depth from CRUST 1.0 model (Fig. 12a). CRUST 1.0 is the only available digital data of the study area. The Moho depth of the CRUST 1.0 model area is calculated using seismic data. The CRUST 1.0 Moho depth is available at 1×1 degrees, so we resampled at our Moho map's same resolution. The difference between the CRUST 1.0 Moho and our estimates is presented in Fig. 12b. The depth of CRUST 1.0 appears to be smoothed over wide geographic regions, which yields a constant Moho over the Great Basin and Wyoming craton. The depth difference was calculated arithmetically by subtracting the CRUST 1.0 Moho depth from the Moho depth of our estimates. The standard deviation of the misfit is 1.43 (Fig. 12c), which shows the closeness of our estimates with the previous estimates.

Moreover, we visually inspected the correlation between our results and the previous estimates of (Gilbert, 2012) and (Ma and Lowry, 2017). The depth estimates of this literature are not available in digital format,

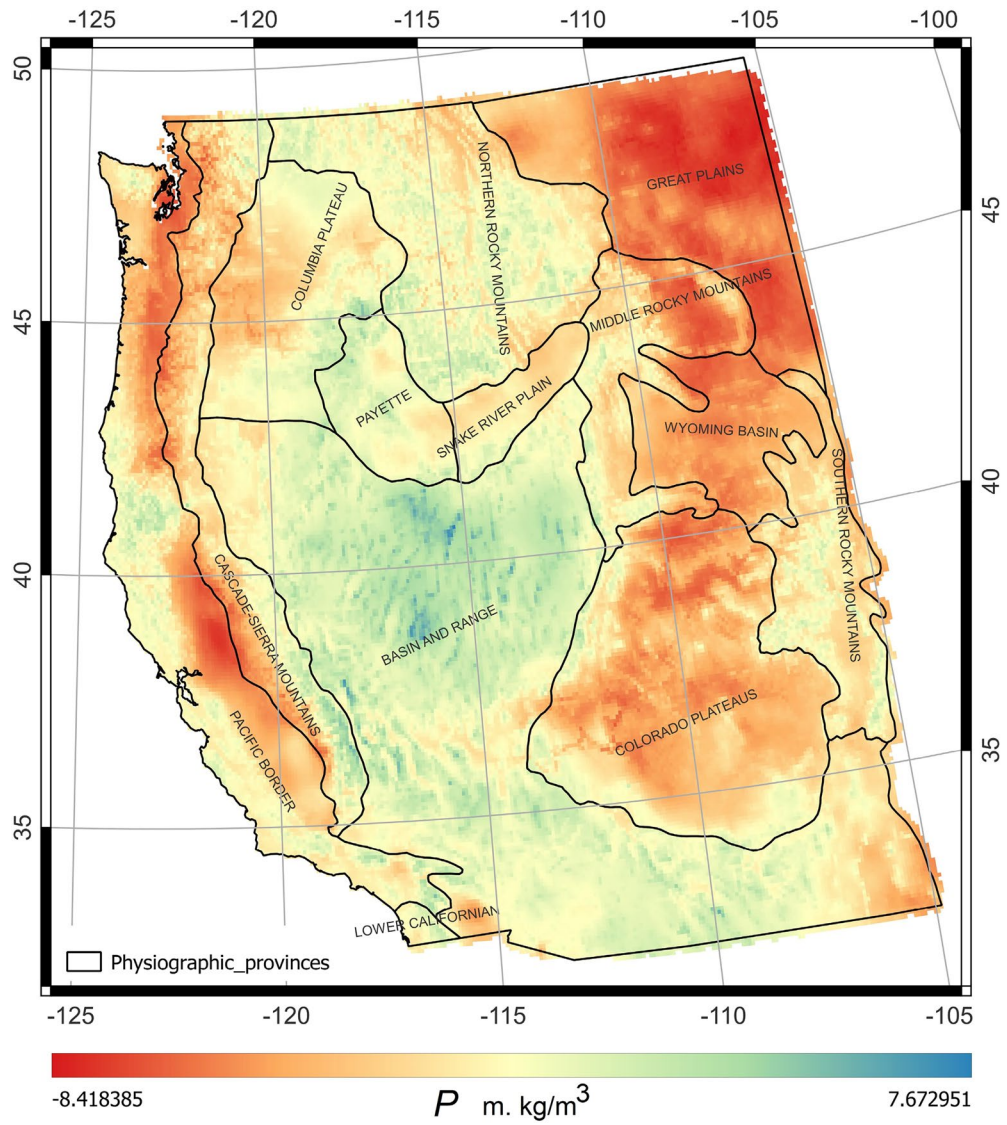

Fig. 9 Compensation Load, *P*, in the study area

so we visually correlated our results with this literature. The seismic estimates of Gilber (2012) show a wide area of no estimates (white regions) due to the absence of seismic data in these regions (Fig. 13a). The seismic estimates of Ma and Lowry (2017) show almost the same depth distribution as the CRUST 1.0 model, where the Moho depth is smoothed (interpolated) over wide geographic regions (Fig. 13b).

Discussion summary

We used gravity data to determine the depth of Moho to examine the tectonic implications of the western United States. The research area's Moho depth has a high geographical association with the study area's physiographic provinces. Moho depth shows a shallowing tren westward near the active tectonic margin at the Pacific border, while the stable craton at the east shows a deep Moho reaching 50 km.

The tectonic implications of Moho appear clearly in the crustal compensation load; an extra compensating force occurs inside the crust and topmost mantle. These loads reveal isostatic correction for large-scale crustal structures.

The origin of topography in the research region shows a significant contribution from the crust as the crustal topography of the southern Rockies and Wyoming craton,

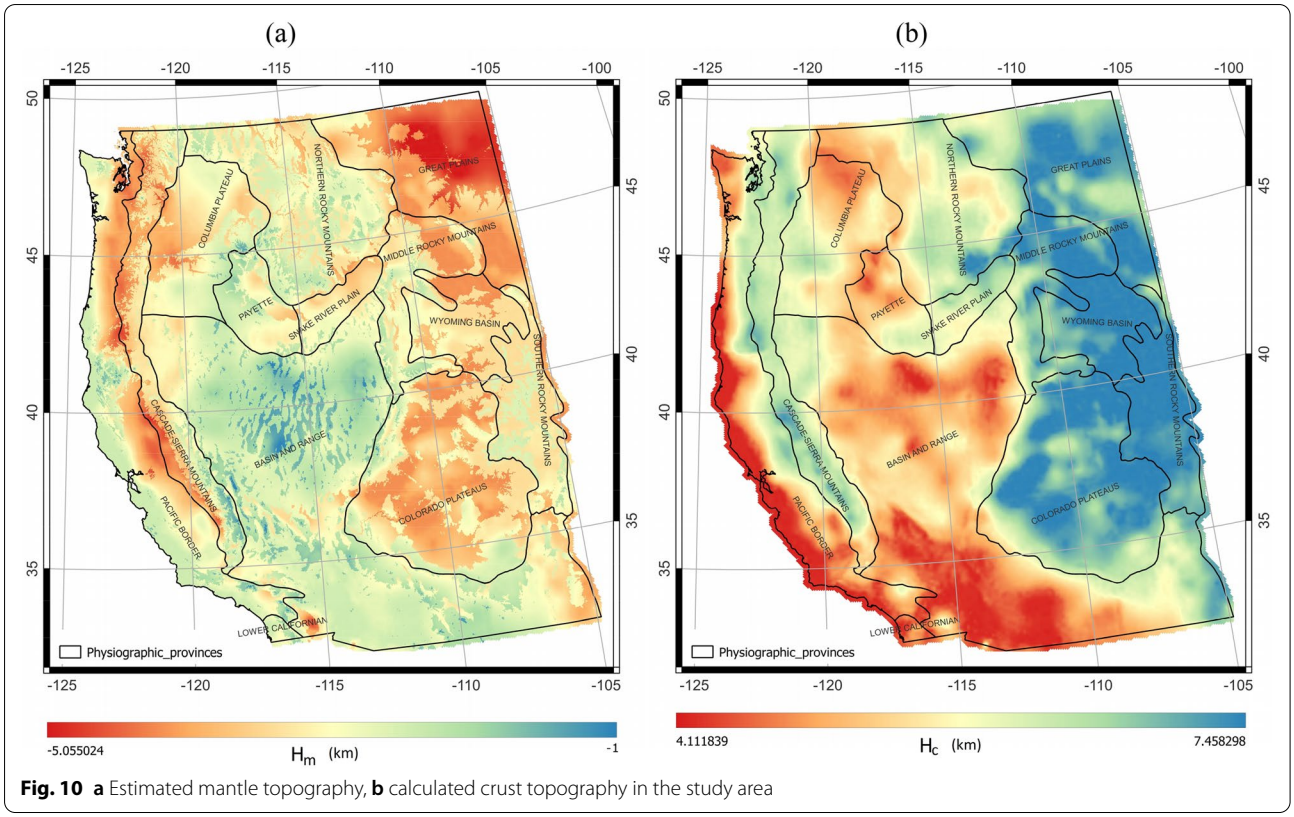

Fig. 10 **a** Estimated mantle topography, **b** calculated crust topography in the study area

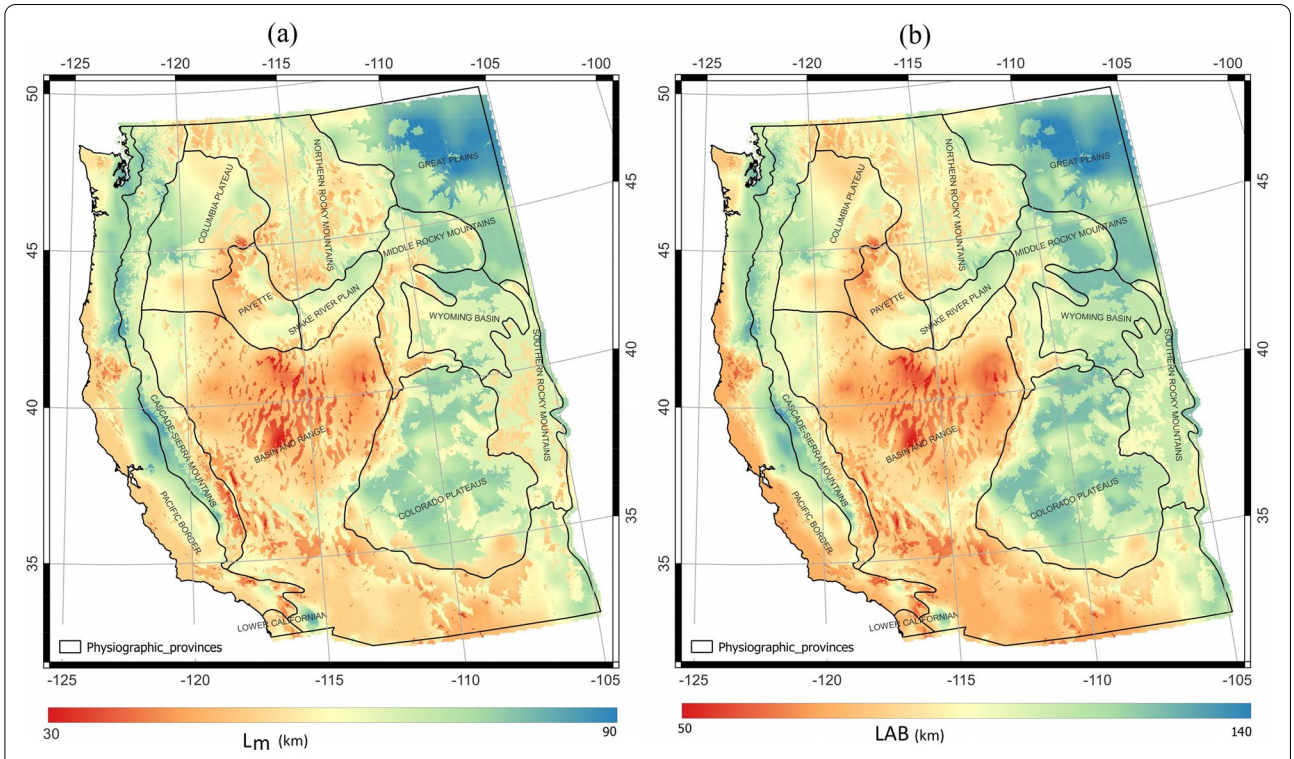

Fig. 11 **a** Calculated mantle–lithosphere thickness, **b** calculated depth to the Lithosphere–Athsenosphere Boundary (LAB) in the study area

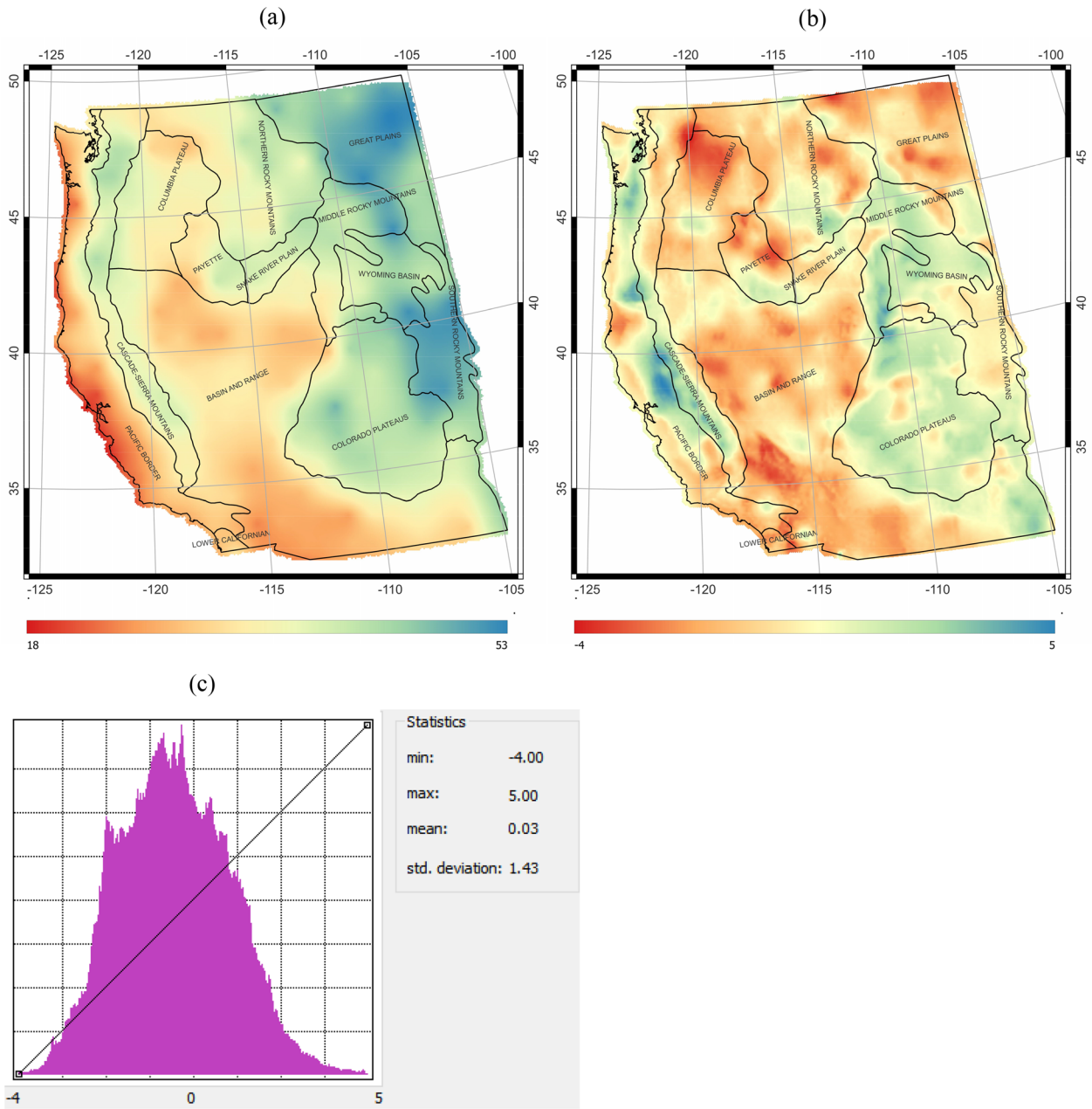

Fig. 12 **a** Moho depth (km) from CRUST 1.0 model, **b** calculated misfit map (km) between our estimates of Moho and CRUST 1.0 model in the study area, **c** misfit between the estimated Moho depths from gravity inversion and Moho depths from the CRUST 1.0 model

on the other hand, indicates a considerable amount of support. In contrast, mantle topography shows negative values in the Wyoming Craton and Great Plains. The thickness of the lithospheric mantle and the depth of LAB show a correlation between the physiographic provinces of the study area.

The correlation analysis between our estimates and previous estimates of Moho depth in the study area shows that in terms of accuracy, our estimates have a reasonable correlation with a difference of ± 4 on average when compared to seismic estimates with a standard deviation of 1.43. Significantly, our estimates provide a more precise lateral mapping efficiency than other geophysical estimates. Our results can be used as a reference base model for the Moho depth in the study area, which enables a better mapping of the lithospheric structure when integrated with other geophysical data.

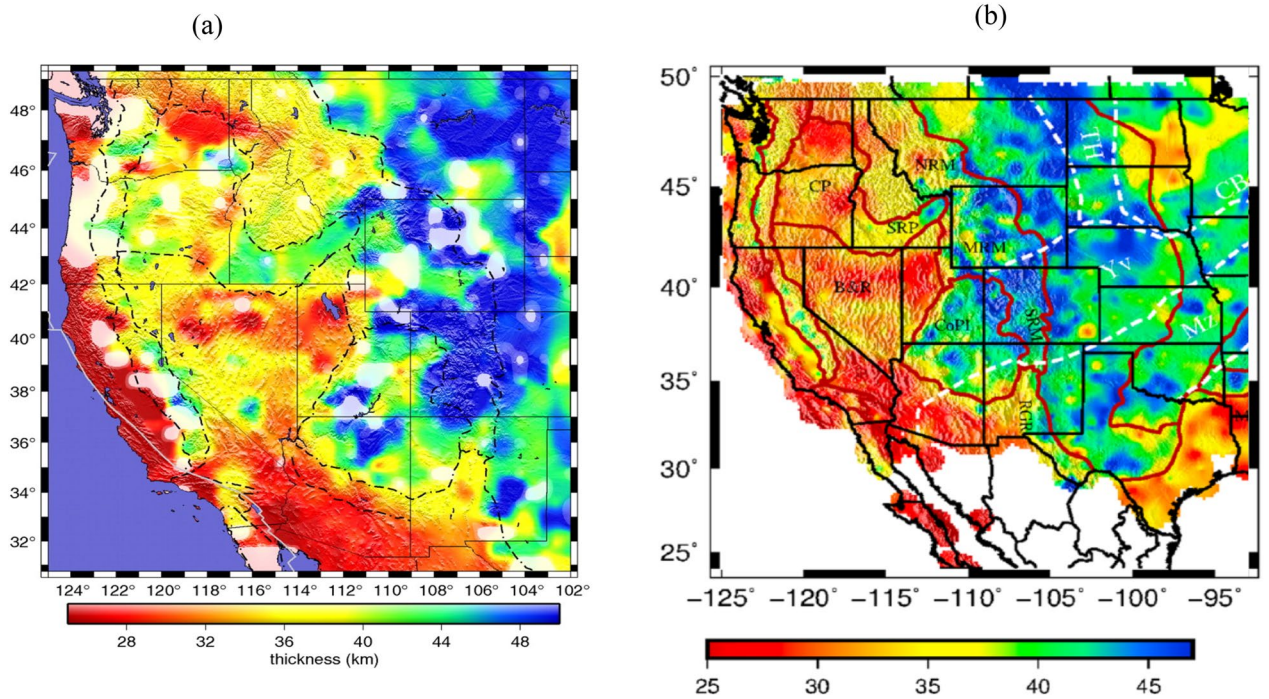

Fig. 13 Estimated Moho depth of the study area sing seismic data: **a** Gilbert (2012) and **b** Ma and Lowry (2017)

Conclusions

The study area, wester U.S., represents the central part of the Western Cordillera. The effect of active tectonism in this area appears clearly in the topography, earthquakes, and volcanism throughout the geologic history. Geophysical data of the study area is available at low spatial resolution yielding a vouge estimate of the Moho depth and LAB. On the other hand, Gravity data is available with high measuring density, allowing precise subsurface mapping. We acquired the dense gravity of the study area and applied Parker–Oldnbuge to estimate the depth to Moho. The estimated Moho depth shows an excellent spatial correlation with physiographic provinces in the study area with an eastward depth increment. We compared our estimates of Moho depth with previous estimates; the results show a good correlation confirming the efficiency of the gravity data and the utilized algorithm to map the Moho at a sub-continental scale with a high spatial resolution compared with other geophysical data. The estimated Moho depth can be used as a reference baseline for further geophysical investigation in the study area at a regional or local scale.

Acknowledgements
We thank the Ministry of Higher Education, Egypt, for supporting the first author to participate in this research through a study grant. In addition, the authors thank the Bureau Gravimetrique International (BGI) for providing the gravity data of the study area.

Author contributions
Conceptualization, MS; data curation, MS; formal analysis, MS; investigation, MS; methodology, MS; software, MS; supervision, HM; validation, MS; visualization, MS; writing—original draft, MS; writing—review and editing, HM. Both authors read and approved the final manuscript.

Funding
This paper does not build directly on a contemporary grant.

Availability of data and materials
The data sets used and analyzed during the current study are available from the corresponding author upon reasonable request.

Declarations

Competing interests
The authors declare that they have no competing interests.

Author details
[1]Department of Earth Resources Engineering, Faculty of Engineering, Kyushu University, Fukuoka 819-0395, Japan. [2]Department of Geology, Faculty of Science, Port Said University, Port Said 42522, Egypt.

Received: 23 March 2022 Accepted: 13 June 2022
Published online: 27 June 2022

References

Buehler JS, Shearer PM (2010) Pn tomography of the western United States using USArray. J Geophys Res Solid Earth. https://doi.org/10.1029/2009JB006874

Chakraborty K, Agarwal BNP (1992) Mapping of crustal discontinuities by wavelength filtering of the gravity field. Geophys Prospect 40:801–822
DePaolo DJ, Cerling TE, Hemming SR, Knoll AH, Richter FM, Royden LH, Trefil JS (2008) Origin and evolution of earth: research questions for a changing planet. National Academies Press, Washington, DC
Dickinson WR (2004) Evolution of the North American Cordillera. Annu Rev Earth Planet Sci 32:13–45
Dickinson WR, Snyder WS (1978) Plate tectonics of the Laramide orogeny, in Matthews, V., III, ed., Laramide folding associated with basement block faulting in the western United States. Geol Soc Am Mem 151:355–366
Dueker KG, Sheehan AF (1997) Mantle discontinuity structure from midpoint stacks of converted P to S waves across the Yellowstone hotspot track. J Geophys Res Solid Earth 102(B4):8313–8327
Eagar KC, Fouch MJ, James DE, Carlson RW (2011) Crustal structure beneath the High Lava Plains of eastern Oregon and surrounding regions from receiver function analysis. J Geophys Res Solid Earth. https://doi.org/10.1029/2010JB007795
Farag T, Sobh M, Mizunaga H (2022) 3D constrained gravity inversion to model Moho geometry and stagnant slabs of the Northwestern Pacific plate at the Japan Islands. Tectonophysics 829:229297
Gilbert H (2012) Crustal structure and signatures of recent tectonism as influenced by ancient terraces in the western United States. Geosphere 8(1):141–157
Gorman AR, Clowes RM, Ellis RM, Henstock TJ, Spence GD, Keller GR, Miller KC (2002) Deep Probe: imaging the roots of western North America. Can J Earth Sci 39(3):375–398
Hansen S, Dueker K (2009) P-and S-wave receiver function images of crustal imbrication beneath the Cheyenne Belt in southeast Wyoming. Bull Seismol Soc Am 99(3):1953–1961
Jones CH, Wernicke BP, Farmer GL, Walker JD, Coleman DS, McKenna LW, Perry FV (1992) Variations across and along a major continental rift: an interdisciplinary study of the Basin and Range Province, western USA. Tectonophysics 213(1–2):57–96
Kaban MK, Mooney WD (2001) Density structure of the lithosphere in the southwestern United States and its tectonic significance. J Geophys Res Solid Earth 106(B1):721–739
Lachenbruch AH, Morgan P (1990) Continental extension, magmatism, and elevation; formal relations and rules of thumb. Tectonophysics 174(1–2):39–62
Lefort JP, Agarwal BNP (2000) Gravity and geomorphological evidence for a large crustal bulge cutting across Brittany (France): a tectonic response to the closure of the Bay of Biscay. Tectonophysics 323:149–162
Levander A, Miller MS (2012) Evolutionary aspects of lithosphere discontinuity structure in the western US. Geochem Geophys Geosystems. https://doi.org/10.1029/2012GC004056
Li G, Bidgoli TS, Chen M, Ma X, Li J (2022) Sedimentary and crustal structure of the western United States from joint inversion of multiple passive seismic datasets. J Geophys Res Solid Earth 127(2):e2021JB022384
Lin FC, Tsai VC, Schmandt B (2014) 3-D crustal structure of the western United States: application of Rayleigh-wave ellipticity extracted from noise cross-correlations. Geophys J Int 198(2):656–670
Ma X, Lowry AR (2017) USArray imaging of continental crust in the conterminous United States. Tectonics 36(12):2882–2902
Oldenburg DW (1974) The inversion and interpretation of gravity anomalies. Geophysics 39(4):526–536
Ostopowich M (2006) The Cordillera. DIANE Publishing Inc, Collingdale
Parker RL (1973) The rapid calculation of potential anomalies. Geophys J Roy Astron Soc 31:447–455
Rao DB, Babu NR (1991) A rapid method for three-dimensional modeling of magnetic anomalies. Geophysics 56(11):1729–1737
Saager R, Bianconi F (1971) The mount Nansen gold-silver deposit, Yukon Territory. Canada Mineralium Deposita 6(3):209–224
Smith RB, Braile LW (1994) The Yellowstone hotspot. J Volcanol Geoth Res 61(3–4):121–187
Telford WM, Geldart LP, Sheriff RE (1990) Applied geophysics. Cambridge University Press, Cambridge, p 792
Tsuboi C (1983) Gravity, 1st edn. George Allen & Unwin Ltd, London, p 254
Williams, M. L., Fischer, K. M., Freymueller, J. T., Tikoff, B., and Tréhu, A. M. (2010). Unlocking the secrets of the North American Continent: An EarthScope Science Plan for 2010–2020, p 78
Zoback ML, Thompson GA, Anderson RE (1981) Cainozoic evolution of the state of stress and style of tectonism of the Basin and Range province of the western United States. Philos Trans Royal Soc A Math Phys Sci 300(1454):407–434

Publisher's Note